Journal of Hazardous Materials 177 (2010) 668–675

Contents lists available at ScienceDirect

Journal of Hazardous Materials

journal homepage: www.elsevier.com/locate/jhazmat

Adsorption of Remazol Black 5 from aqueous solution by the templated crosslinked-chitosans

Arh-Hwang Chen*, Yao-Yi Huang

Department of Chemical and Materials Engineering, Southern Taiwan University, No. 1, Nantai St., Yungkang, Tainan 710, Taiwan, ROC

ARTICLE INFO

Article history:
Received 2 September 2009
Received in revised form
23 November 2009
Accepted 17 December 2009
Available online 24 December 2009

Keywords:
Adsorption
Remazol Black5
Templated crosslinked-chitosan
Competition
Regeneration

ABSTRACT

The templated crosslinked-chitosan microparticles prepared using the imprinting method with the Remazol Black5 (RB5) dye as a template, epichlorohydrin (ECH) as a crosslinker, and sodium hydroxide (NaOH) solution used for the microparticle formation showed the highest adsorption capacity for the RB5 dye compared with those that used other methods with or without a template, three crosslinkers, and two microparticle formations. The results showed that the adsorption of the RB5 dye on the microparticles was affected by the microparticle size, the initial dye concentration, the initial pH value, as well as the temperature. Both kinetics and thermodynamic parameters of the adsorption process were estimated. These data indicated an exothermic spontaneous adsorption process that kinetically followed the second-order adsorption process. Equilibrium experiments fitted well the Langmuir isotherm model, and the maximum monolayer adsorption capacity for the RB5 dye was 2941 mg/g. The competition study showed that the adsorption of the RB5 dye on the microparticles in the mixture solution was much less affected by the existence of the 3R dye than the other way around. Furthermore, the microparticles could be regenerated through the desorption of the dye in pH 10.0 of NaOH solution and could be reused to adsorb the dye again.

© 2009 Elsevier B.V. All rights reserved.

1. Introduction

It is known that dyestuff in wastewater from various industries such as dyestuff, textile, leather, paper, and plastics is difficult to remove, because it has recalcitrant molecules (particularly azo dyes with an aromatic structure), is resistant to aerobic digestion, and is stable to oxidizing agents. Hence, the removal of dyestuff from waste effluents becomes environmentally important. A wide range of conventional treatment processes including coagulation, precipitation, biodegradation, oxidation, membrane separation, adsorption, and photodegradation has been utilized for removing dyestuffs from wastewater [1,2]. From these applied methodologies to purify effluents, adsorption seems to be a reliable alternative, and many adsorbents have been proposed for this purpose.

Various natural or synthetic materials have been tested, and currently chitosan is being greatly exploited owing to its advantages when compared, for example, with active carbon, which is the most intensively used material. Indeed, the success of chitosan is closely related to its adsorption capacity, which mainly uses the available amino and hydroxy groups. Thus, chitosan has been considered as one of the most popular adsorbents for the removal of metal ions, dyes, and proteins from an aqueous solution and has been widely used in waste treatment applications, because it has been proven to have better chelating power than other biopolymers [3–7]. However, the amino groups of chitosan are fully protonated at about pH 3.0, and the polymer chains with positive charges fall apart in the solution resulting in dissolution in an acidic medium. Hence, the crosslinking reactions of chitosan including epichlorohydrin (ECH), glutaraldehyde (GLA), and ethylene glycol diglycidyl ether (EGDE) as crosslinkers have been used to improve its chemical stability in any acid media, and its selectivity and capacity for the adsorption of dyes from industrial effluents [8–12]. Although the crosslinking method may enhance the resistance of chitosan against acids, the process may reduce its adsorption capacity of dyes. This may be attributed to the fact that the crosslinking reaction decreases the amount of amino and hydroxyl groups, which are expected to play a great part in the adsorption process.

To overcome this drawback, this study was developed to synthesize the templated crosslinked-chitosans using the imprinting method, which is similar to the process for the preparation of molecularly imprinted polymers [13,14]. It used the Remazol Black5 (RB5) dye as a template for chelating with chitosan, and then crosslinked with three crosslinkers: ECH, GLA, and EGDE. The microparticle formation was carried out in sodium hydroxide (NaOH) or sodium tripolyphosphate (TPP) solutions. Finally, the microparticles were removed the dye template and were used for the adsorption of the RB5 dye in an aqueous medium. Furthermore, the initial pH effect, kinetics, equilibrium, competition, desorption

* Corresponding author. Tel.: +886 6 2533131x6937; fax: +886 6 2432846.
E-mail address: chenah@ms12.hinet.net (A.-H. Chen).

0304-3894/$ – see front matter © 2009 Elsevier B.V. All rights reserved.
doi:10.1016/j.jhazmat.2009.12.083

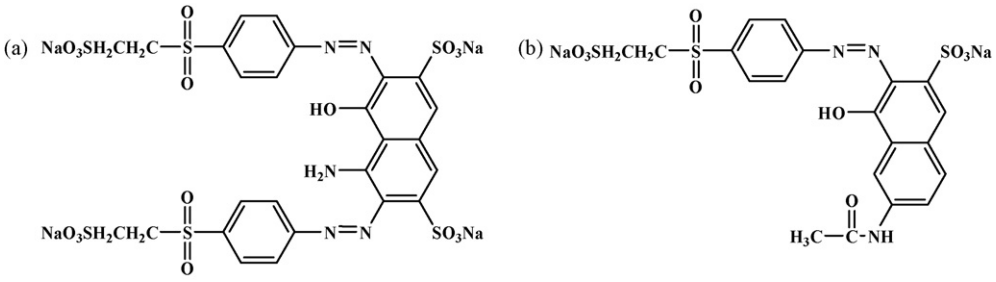

Fig. 1. The structures of (a) Remazol Black 5 (RB5) and (b) Remazol Brilliant Orange 3R (3R).

and reuse were examined for better comparison of the experimental results. This information would be useful for further applications in the treatment of waste effluents in the dye industry.

2. Materials and methods

2.1. Chemicals

Chitosan was purchased from Sigma–Aldrich Co., USA. It was then hydrolyzed with sodium hydroxide to give it a deacetylation percentage of approximately 90% following the Fourier transform infrared (FTIR) methods. The average molecular weight was 690,000 as measured through the viscometric method. Remazol Black5 (RB5), Remazol Brilliant Orange 3R (3R), epichlorohydrin (ECH), glutaraldehyde (GLA), ethylene glycol diglycidyl ether (EGDE) and sodium tripolyphosphate (TPP) with 55, 50, 99, 50, 50, and 85% purities, respectively, were purchased from Sigma–Aldrich Co., USA. All the reagents were used without undergoing further purification. The structures of the RB5 and 3R dyes are presented in Fig. 1.

2.2. Preparation

The templated crosslinked-chitosans were prepared using the imprinting method. A solution was prepared with 0.125 g of chitosan dissolved into a 25 mL aqueous solution of acetic acid (1%, v/v). A 5.0 mL aqueous solution of the RB5 dye (1.45 mM) was added, and the mixture was stirred for 30 min. Afterwards, a 25.0 mL aqueous solution of ECH was added dropwise, after which the mixture was stirred for 2 h at 50 °C. Subsequently, the chitosan solution was slowly dropped using a syringe into 25 mL of 0.5 M NaOH solution with mechanical stirring to form the microparticle precipitates. The process was followed by filtering and intensive washing of the precipitate with distilled water to remove any unreacted ECH. The precipitate was again stirred, this time with a pH 10.0 NaOH solution to remove the dye. This stage was monitored with an UV/visible spectrophotometer and was subsequently mixed with a 1% (v/v) acetic acid to remove non-crosslinking chitosan. The precipitates were filtered out and washed with distilled water and acetone. They were then dried inside a vacuum oven at 50 °C for 8 h. The resulting materials were sieved to collect the particles with three different diameter sizes: 149–250 μm, 250–500 μm, and 500–1000 μm, all of which were later used for this study.

The FTIR spectra of the microparticles were determined using the pressed-disk method with potassium bromide on a Perkin Elmer Spectrum One FTIR spectrometer. The solid state ^{13}C nuclear magnetic resonance spectra of the materials were measured on a Brucker Advance 400 NMR spectrometer. The SEM photomicrograph of the microparticles was taken using a JEOL JSM-6700F scanning electron microscopy. The mean pore diameters of the materials were measured on a mercury intrusion porosimeter Scientek STK019348.

2.3. Dye adsorption

The templated microparticles (diameter: 149–250 μm) prepared from different molar ratios of crosslinker/chitosan were studied to determine the adsorption capacity of the RB5 dye. This process was carried out by adding a 10 mg of each kind of the templated microparticles into a 10 mL of 4.0 mg/mL dye solution at pH 3.0 while stirring at 30 °C for 120 h. The solution was filtered through Millipore 0.45 μm HV filter paper and adjusted to a pH level of 6.0 using HCl or NaOH solutions. The dye concentration was measured using an UV/visible spectrophotometer, Shimadzu UV-2401 PC, at 597 nm, while the adsorption capacity (Q) (mg/g) was calculated using Eq. (1):

$$Q = \frac{(C_i - C_f)V}{W} \quad (1)$$

where C_i is the initial concentration of dye (mg/mL); C_f is the final concentration of dye (mg/mL); V is the volume of dye solution (mL); W is the weight of the chitosan microparticles (g) used.

2.4. Batch kinetics

The adsorption kinetics of the RB5 dye on the templated ECH–RB5–NaOH microparticles (diameter: 149–250 μm) was carried out in a batch process. The variable parameters were studied, including the initial concentrations of dye, initial pH values, and temperatures. In each test, 10 mg of the microparticles was conducted in 10 mL of aqueous solution of dye with a known concentration. Whenever necessary, the pH value was adjusted with dilute NaOH or HCl solutions. Afterwards, 0.1 mL aliquots of the solution at different time intervals were added to 5 mL distilled water. The mixture was filtered through Millipore 0.45 μm HV filter paper, adjusted to pH 6.0, and then diluted into 10 mL. The concentrations of dye were measured using an UV/visible spectrophotometer. The amount of adsorption was calculated using Eq. (1).

To determine the rate-controlling and mass transfer mechanism, kinetic data were correlated to linear forms of the first-order equation (2):

$$\ln(Q_e - Q_t) = \ln Q_e - k_1 t, \quad (2)$$

and the second-order equation (3):

$$\frac{t}{Q_t} = \frac{1}{k_2 Q_e^2} + \frac{t}{Q_e}, \quad (3)$$

where Q_e and Q_t are the adsorption capacities of dye (mg/g) at equilibrium and at a given time t, respectively; k_1 (min^{-1}) and k_2 (g/(mg min)) are the first-order and the second-order rate constants, respectively. According to Eq. (2), the plot of $\ln(Q_e - Q_t)$ versus t gives a straight line with a slope of $-k_1$ and an intercept of $\ln Q_e$. From Eq. (3), the plot of t/Q_t versus t gives a straight line with a slope of $1/Q_e$ and an intercept of $1/(k_2 Q_e^2)$.

2.5. Batch equilibrium

The equilibrium studies were carried out by suspending 10 mg of the templated ECH–RB5–NaOH microparticles (diameter: 149–250 μm) in 10 mL of initial dye concentrations within the range of 0.1–5.0 mg/mL at pH 3.0 and with stirring for 120 h at 30 °C. The solutions were filtered, adjusted to pH 6.0, and then diluted to 10 mL. The concentrations of dye were measured using an UV/visible spectrophotometer. In accordance with Eq. (1), the amount of adsorption was then calculated based on the differences of the concentration in an aqueous solution (10 mL) before and after the adsorption, as well as on the weight of the microparticles (0.010 g) themselves.

2.6. Competition study

Assuming there is no interaction between the two dyes (RB5 and 3R), the total absorbance for a mixture dye solution is equal to the summation of the absorbance of each dye, which is represented by Eq. (4). The adsorption capacity of each dye in a mixture solution can be calculated using Eqs. (5) and (6):

$$A_\lambda = A_{RB5} + A_{3R} \quad (4)$$

$$A_{\lambda 1} = \varepsilon_{1RB5} L C_{RB5} + \varepsilon_{13R} L C_{3R} \quad (5)$$

$$A_{\lambda 2} = \varepsilon_{2RB5} L C_{RB5} + \varepsilon_{23R} L C_{3R} \quad (6)$$

where A_λ, $A_{\lambda 1}$ and $A_{\lambda 2}$ are the absorbance of UV/visible spectrometer at wavelength λ, λ_1 and λ_2, respectively; A_{RB5} and A_{3R} are the absorbance of RB5 and 3R at wavelength λ, respectively; ε_{1RB5} and ε_{2RB5} are the molar absorptivities of pure RB 5 at wavelength λ_1 and λ_2, respectively; ε_{13R} and ε_{23R} re the absorbance coefficients of pure 3R at wavelength λ_1 and λ_2, respectively; C_{RB5} and C_{3R} are the concentrations of RB5 and 3R in the mixture solution, respectively; L is the cell with (1 cm); and λ_1 (597 nm) and λ_2 (494 nm) are the wavelengths of maximum absorbance for RB5 and 3R, respectively. The concentrations of C_{RB5} and C_{3R} are calculated from Eqs. (5) and (6). Hence the adsorption capacity of each dye in the mixture solution can be obtained.

3. Results and discussion

3.1. Characterization and dye adsorption

As shown in Fig. 2, using the imprinting method, the chitosan was first chelated with RB5 dye as a template, followed by chemically crosslinking with three crosslinkers (ECH, GLA, and EGDE), for example, epichlorohydrin via an ether linkage. The microparticle formation was conducted in NaOH or TPP solutions and finally the microparticles were removed the dye template to give the templated crosslinked-chitosans. The microparticles were revealed to be insoluble in distilled water, alkaline medium, and even in acidic medium (pH 1.0). The templated crosslinked-chitosan microparticles prepared from the three crosslinkers with 0.50 molar ratio of crosslinker/chitosan were characterized using the FTIR. The microparticles formed from the NaOH solution showed an absorption peak for amide C=O and/or imine C=N stretching vibrations at 1658 cm^{-1}, which were dependent on the crosslinker used, and another absorption peak for amide N–H bending vibration at 1575 cm^{-1} [15]. However, the microparticles formed from the TPP solution had an intense absorption peak of 1535 cm^{-1}, which accounted for the tripolyphosphate ions ($P_3O_{10}^{5-}$). The solid state ^{13}C NMR of the templated crosslinked-chitosans with ECH appeared to have three peaks at 61.6, 85.0, and 97.6 ppm due to exiting of –O–CH_2–CHOH–CH_2–O– linkage between two chitosan molecules in comparison with chitosan. The SEM photomicrograph of the ECH–RB5–NaOH microparticles prepared from 0.5 molar ratio of the ECH/chitosan, RB5 dye as a template, and NaOH for the microparticle formation showed that the particles were assembled on the surface (Fig. 3).

The adsorption of the RB5 dye on the templated microparticles prepared from different molar ratios of crosslinker/chitosan and different methods of the microparticle formation were used for the adsorption of the RB5 dye were found to have the maximum adsorption capacities for the RB5 dye at the 0.5 molar ratio of the crosslinker/chitosan (Fig. 4). In addition, the microparticles formed using NaOH solution were shown to have a higher adsorption capacity of the RB5 dye compared with those formed using TPP solution. This may be attributed to the anionic repulsion between the microparticles with tripolyphosphate ions and the dyes with sulfonate ions. The microparticles of ECH–RB5–NaOH prepared from 0.5 molar ratio of the ECH/chitosan, RB5 dye as a template, and NaOH for the microparticle formation showed the highest adsorption capacity for the RB5 dye compared with the chitosan microparticles formed with two microparticle formations (NaOH or TPP) and the microparticles prepared with or without template, three crosslinkers (GLA, ECH or EGDE) and two microparticle formations (NaOH or TPP). This may be attributed to the fact that the mean pore diameter of ECH–RB5–NaOH microparticles (27.87 μm) was larger than that of other microparticles, such as GLA-RB5-NaOH (23.13 μm) and EGDE-RB5-NaOH (23.80 μm), measured using the mercury intrusion porosimetry.

3.2. Adsorption kinetics and thermodynamics

The effects of the initial pH for the adsorption kinetics of the RB5 dye on the ECH–RB5–NaOH microparticles at 4.0 mg/mL initial dye concentration and 30 °C were shown in Fig. 5(a). The pH values were monitored before and after the adsorption of dyes with pH differences from only 0.1 to 0.2. The adsorption capacity was decreased by 23.2% from 2565 to 1969 mg/g with the increase of the initial pH of solution from 1.0 to 6.0. This may be attributed to the fact that at a lower pH solution, more protons are available to protonate the amino groups of chitosan molecules to form $-NH_3^+$ groups; this increases the electrostatic attraction between the anionic group ($-SO_3^-$) of the dye and the protonated amino group ($-NH_3^+$) of chitosan, causing an increase in dye adsorption [16].

Fig. 5(b) shows the influences of the initial dye concentration for the adsorption kinetics of the RB5 dye on the ECH–RB5–NaOH microparticles at pH 3.0 and 30 °C. As the increase of the initial dye concentration from 3.0 to 6.0 mg/mL, the dye adsorption capacity was increased by 32.6% from 1834 to 2720 mg/g. The initial dye concentration provides an important driving force to overcome the mass transfer resistance of the dye between aqueous and solid phases. Hence, the adsorption of the dye increases with the increase in the initial dye concentration. At first, the adsorption rate may be higher because of an increase in the number of vacant sites initially available, resulting in an increased concentration gradient between the sorbate in the solution and that at the sorbent surface. In time, the concentration gradient is reduced owing to the adsorption of the dye molecules onto the vacant sites, leading to decreased adsorption during the later stages [17].

By correlation of the kinetic data from different initial pH values, different initial dye concentrations, and different temperatures with the first-order and the second-order kinetic equations (Table 1), it was found that the correlation coefficients, R^2, from the second-order adsorption kinetics were higher than those from the first-order kinetics. In addition, the calculated equilibrium adsorption capacities, $Q_{e,cal}$, from the second-order kinetics fitted well with the experimental data. This indicated that the adsorption process followed predominantly the second-order rate model, and the overall process appeared to be controlled by chemisorption. It may

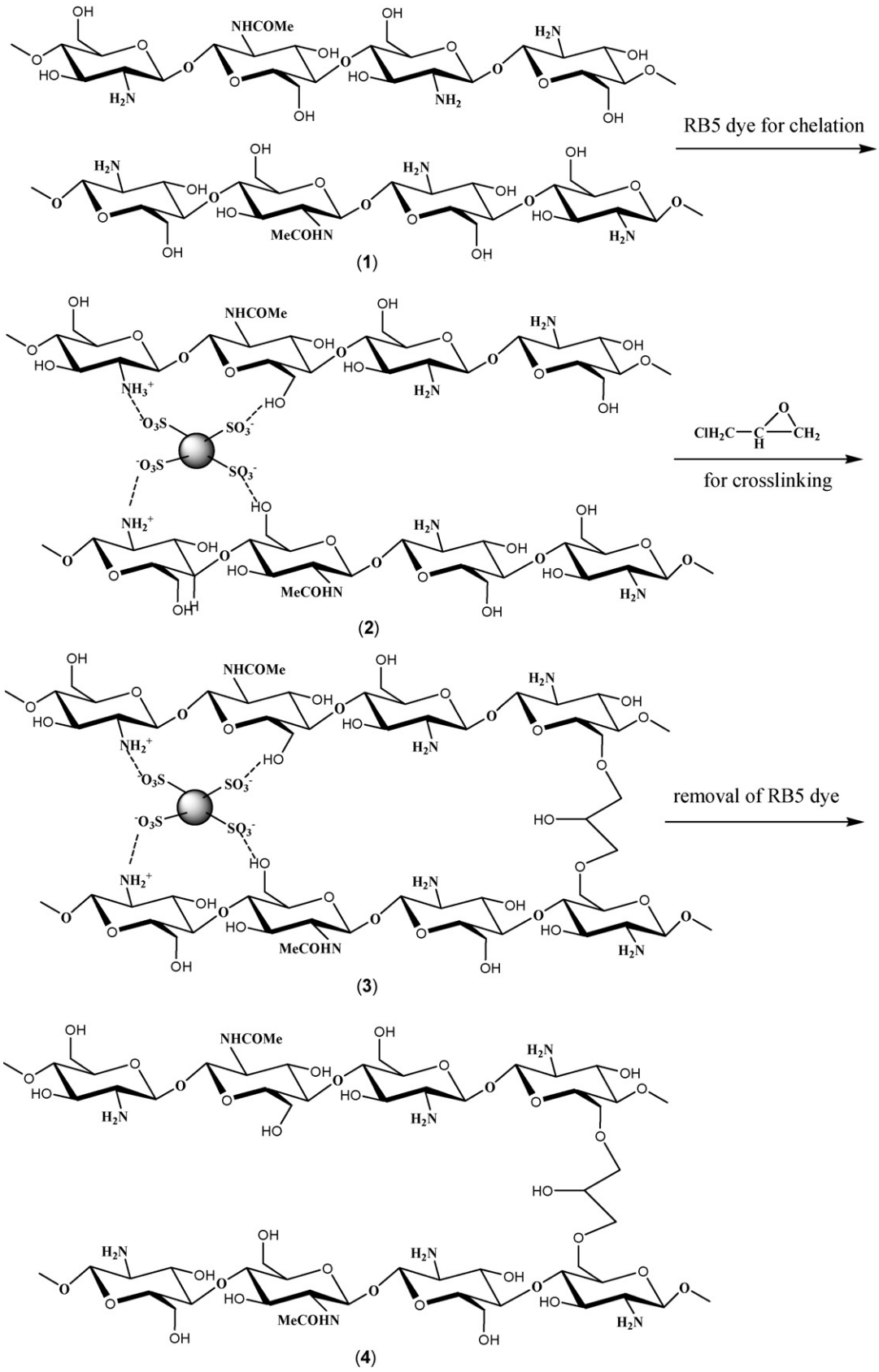

Fig. 2. Schematic representation for preparation process of the templated crosslinked-chitosans with epichlorohydrin.

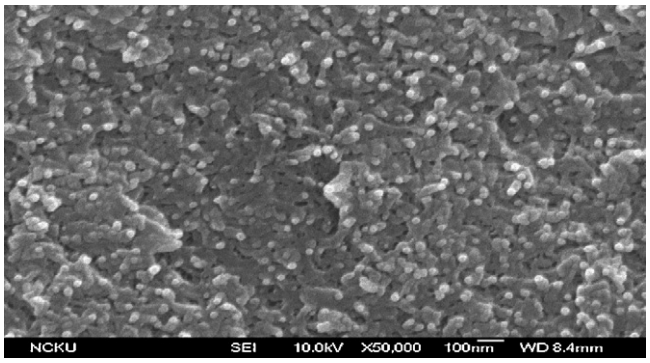

Fig. 3. SEM photomicrographs of the microparticles of ECH–RB5–NaOH prepared from 0.5 molar ratio of the ECH/chitosan, RB5 dye as a template, and NaOH for the microparticle formation.

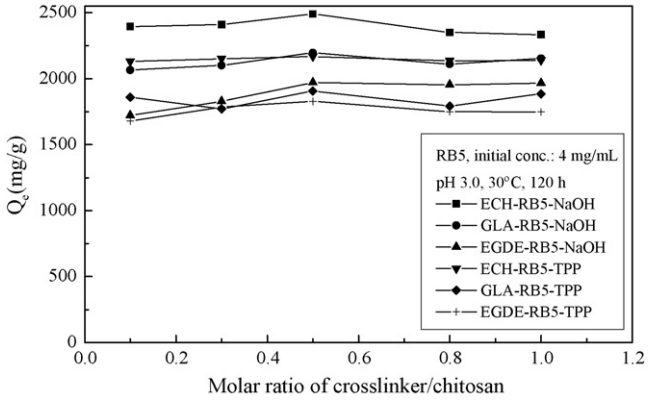

Fig. 4. Adsorption capacity of RB5 dye on the templated crosslinked-chitosans (diameter: 149–250 μm) prepared from different molar ratios of crosslinker/chitosan in 4.0 mg/mL initial concentrations of dye for 120 h at pH 3.0 and 30 °C.

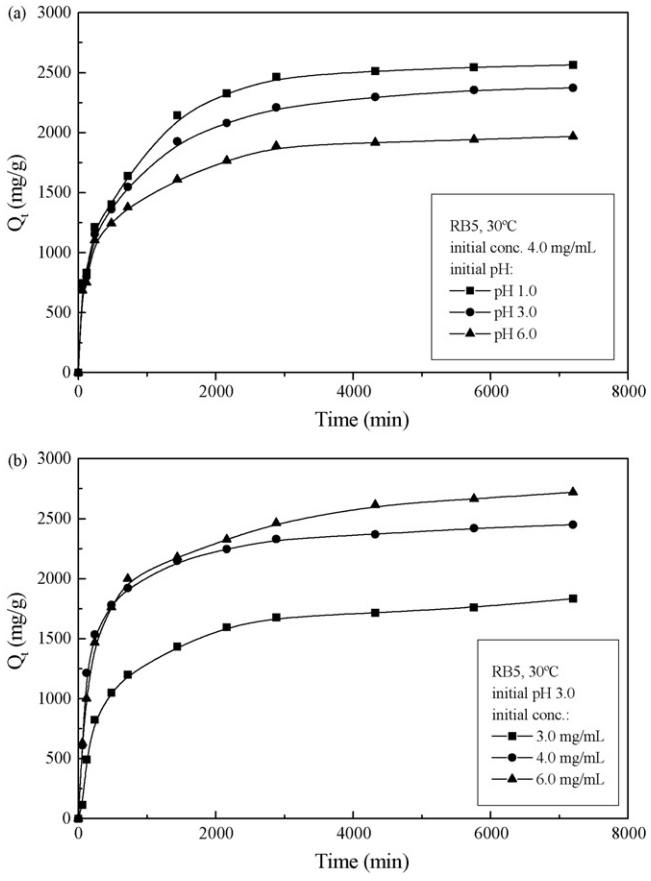

Fig. 5. Absorption kinetics of RB5 dye on the ECH–RB5–NaOH microparticles (diameter: 149–250 μm): (a) different initial pH solutions and (b) different initial concentrations of dye.

be attributed to the fact that the rate-determining step may have involved a valency force through the sharing of electrons between dye anions and adsorbent [5,8].

According to van't Hoff equation, the standard Gibbs free energy change (ΔG°), standard enthalpy change (ΔH°), and standard entropy change (ΔS°) are determined using Eqs. (7) and (8) [18,19]:

$$\ln K_L = \frac{-\Delta H^\circ}{RT} + \frac{\Delta S^\circ}{R} \quad (7)$$

$$\Delta G^\circ = \Delta H^\circ - T\,\Delta S^\circ \quad (8)$$

where K_L is the Langmuir constant; R is the molar gas constant; T is the absolute temperature. The values of ΔH°, and ΔS° at 30–50 °C (−4.75 kJ/mol and 79.90 J/(mol K), respectively) were calculated from the slope and the intercept of the linear plot of $\ln K_L$ versus $1/T$. The values of ΔG° (−28.86, −29.86, and −31.46 kJ/mol) were calculated from Eq. (8) at 30, 40, and 50 °C, respectively. The negative values of ΔG° and ΔH° indicated that the adsorption processes was spontaneous and exothermic. Meanwhile, the positive values of ΔS° indicated the increased randomness during the adsorptions of the dye on the microparticles. This may be attributed to the lib-

Table 1
The first-order and second-order adsorption rate constants, calculated $Q_{e,cal}$ and experimental Q_e values of RB5 dye on the ECH–RB5–NaOH microparticles (diameter: 149–250 μm) with different initial dye concentrations, pHs and temperatures.

Parameter	Q_e (mg/g) (S.D.)	First-order kinetic model			Second-order kinetic model		
		k_1 ($\times 10^{-4}$) (min^{-1}) (S.D.)	$Q_{e,cal}$ (mg/g) (S.D.)	R^2	k_2 ($\times 10^{-7}$) (g/mg min) (S.D.)	$Q_{e,cal}$ (mg/g) (S.D.)	R^2
pH, time = 120 h (4.0 mg/mL, 30 °C)							
1.0	2600 (17.9)	6.00 (0.01)	1439 (10.9)	0.9461	6.76 (0.04)	2500 (0.1)	0.9923
3.0	2420 (0.3)	4.50 (0.71)	1362 (70.3)	0.9643	9.54 (0.06)	2000 (0.1)	0.9917
6.0	2018 (20.7)	5.50 (0.71)	1102 (109.6)	0.9205	12.32 (0.14)	1666 (0.1)	0.9899
Initial dye concentration (mg/mL), time = 120 h (pH 3.0, 30 °C)							
3.0	1896 (31.1)	4.00 (0.01)	1163 (23.1)	0.9371	9.21 (0.47)	2000 (0.1)	0.9977
4.0	2372 (5.6)	5.00 (0.01)	1136 (7.7)	0.8943	9.26 (0.80)	2500 (0.1)	0.9880
6.0	2807 (66.2)	4.50 (0.71)	1537 (44.2)	0.9480	10.52 (5.18)	2500 (0.1)	0.9931
Temperature (°C), time = 120 h (4.0 mg/mL, pH 3.0)							
30	2373 (1.8)	5.00 (0.01)	1173 (4.6)	0.8860	7.39 (0.06)	2500 (0.1)	0.9895
40	2360 (1.8)	5.00 (0.01)	996 (1.9)	0.8454	9.13 (0.1)	2500 (0.1)	0.9926
50	2333 (0.1)	5.00 (0.01)	741 (1.3)	0.7640	15.67 (0.05)	2000 (0.1)	0.9984

Note: S.D. in the parentheses is the standard deviation.

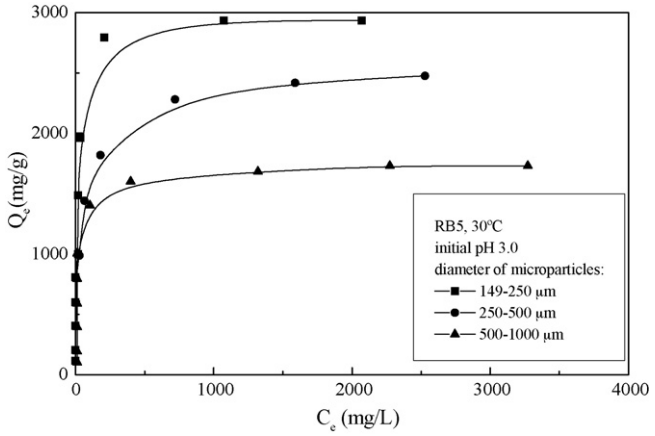

Fig. 6. Equilibrium absorption of RB5 dye on three different sizes of the ECH–RB5–NaOH microparticles at pH 3.0 and 30 °C with different initial concentrations of dye.

eration of water molecules from the hydrated shells of the sorbed species [18].

3.3. Adsorption isotherms

Fig. 6 shows the equilibrium adsorption of the RB5 dye on three different sizes of the ECH–RB5–NaOH microparticles at pH 3.0 and 30 °C with different initial concentrations of dye. The equilibrium adsorption capacity of the dye (Q_e) was increased with the increase in dye concentration. In addition, the adsorption capacity was decreased markedly with the increasing diameter of the microparticle. This may be ascribed to the fact that the adsorption took place mainly on the outer surface of the microparticle owing to the steric hindrance of the dye molecules. The dye adsorption was increased with the decrease in the particle size given that the effective surface area was higher for the same mass of smaller particles.

The adsorption isotherms for the RB5 dye on three different sizes of the microparticles were studied using three isotherm models: Langmuir isotherm equation [20]:

$$\frac{C_e}{Q_e} = \frac{C_e}{Q_m} + \frac{1}{Q_m K_L}, \tag{9}$$

Table 2
Langmuir, Freundlich and Dubinin–Radushkevich isotherm constants for RB5 dye on different particles sizes of the ECH–RB5–NaOH microparticles at pH 3.0 and 30 °C for 120 h.

	Particle sizes (μm)		
	149–250	250–500	500–1000
Langmuir			
Q_m (mg/g) (S.D.)	2941.1 (0.1)	2500.0 (0.1)	1754.1 (0.3)
K_L (L/mg) (S.D.)	0.09 (0.10)	0.06 (0.10)	0.01 (0.10)
R^2	0.9997	0.9994	0.9977
Freundlich			
K_F (mg/g) (S.D.)	493.3 (0.4)	324.0 (0.1)	199.9 (0.2)
b_F (S.D.)	0.27 (0.10)	0.29 (0.10)	0.29 (0.10)
R^2	0.7537	0.8917	0.5334
Dubinnin–Radushkevich			
Q_{DR} (mg/g) (S.D.)	5708.9 (16.1)	5004.5 (8.5)	3729.7 (4.2)
$K \times 10^{-9}$ (J^2/mol^2) (S.D.)	−2.0 (0.1)	−2.0 (0.1)	−2.5 (0.7)
E (kJ/mol) (S.D.)	15.8 (0.1)	15.8 (0.1)	12.9 (0.1)
R^2	0.7734	0.9361	0.5530

Note: S.D. in the parentheses is the standard deviation.

Freundlich isotherm equation [21]:

$$\ln Q_e = b_F \ln C_e + \ln K_F, \tag{10}$$

and Dubinin–Radushkevich isotherm equation [22]:

$$\ln Q_e = K\varepsilon^2 + \ln Q_{DR}, \tag{11}$$

where C_e is the equilibrium concentration of the dye; Q_e is the adsorption capacity of the dye, Q_m, K_F, and Q_{DR} are the Langmuir; Freundlich and Dubinin–Radushkevich maximum adsorption capacities of the dye, respectively; K_L, b_F, and K are the Langmuir, Freundlich and Dubinin–Radushkevich constants, respectively; ε is the Polanyi potential. The Polanyi potential (ε) is given as Eq. (12):

$$\varepsilon = RT \ln\left(1 + \frac{1}{C_e}\right) \tag{12}$$

where R is the gas constant in J/(K mol), and T is the temperate in Kelvin. The Dubinin–Radushkevich constant (K) can give the valuable information regarding the mean energy of adsorption by Eq. (13):

$$E = (-2K)^{-1/2} \tag{13}$$

where E is the mean adsorption energy, and K is the Dubinin–Radushkevich constant. The results were shown in Table 2. The Langmuir isotherm was found to fit quite well with the experimental data for three different microparticles in comparison with the linear correlation coefficients (R^2). The Langmuir maximum adsorption capacity (Q_m) of the RB5 dye on the 149–250 μm microparticles was higher by 40.4% than that on the 500–1000 μm microparticles. In addition, the mean adsorption energy (E) from the Dubinnin–Radushkevich isotherm could involve the transfer of the free energy of one mole of solute from infinity (in solution) to the adsorbent's surface. The adsorption behavior could have predicted the physical adsorption in the range of 1–8 kJ/mol and the chemical adsorption in more than 8 kJ/mol [12,14]. The E values of the RB5 dye from 12.9 to 15.8 kJ/mol indicated that the adsorption process might be due to the dual nature of the process, physisorption and chemisorption, and was predominant on the chemisorption process. Table 3 listed the comparison of the maximum monolayer adsorption capacity (Q_m) of some azo dyes on various adsorbents. The data demonstrated that the microparticles in this work had the higher adsorption capacity for the RB5 dye (2941 mg/g) than those of other adsorbents.

3.4. Competition adsorption

The 3R dye was used for the competition study for the adsorption of the RB5 dye on the ECH–RB5–NaOH microparticles owing to the similar structure of the 3R molecules and the RB5 molecules (Fig. 1). Fig. 7(a) shows the kinetics of the competitive adsorption in the mixture solution of the RB5 and 3R dyes in 4.0 mM initial concentration of each dye at pH 3.0 and 30 °C. As can be seen, the adsorption capacity of the RB5 dye was higher than that of the 3R dye. This may be attributed to the fact that the microparticles had more suitable sites for adsorption of the RB5 molecules than those for the 3R molecules. The ratios for the adsorption capacity of each dye between in the mixture solution of the two dyes and in each single solution with the same initial concentration of each dye were shown in Fig. 7(b). The ratio of RB5 dye was shown to have remained at almost 90%, while the ratio of 3R dye appeared to be less than 60%. Therefore, the adsorption of the RB5 dye on the microparticles in the mixture solution was much less affected by the existence of the 3R dye than the other way around in the competitive adsorption.

Table 3
Comparison of the maximum monolayer adsorption capacity (Q_m) of some azo dyes on various adsorbents.

Azo dye	Adsorbent and method of preparation	Q_m (mg/g)	Reference
Remazol Black 5	Templated ECH-crosslinked-chitosan, homogeneous coupling, using NaOH	2941	This work
Remazol Black 5	GLA-crosslinked-chitosan, homogeneous coupling, using NaOH	1680	[12]
Remazol Brilliant Orange 3R	GLA-crosslinked-chitosan, homogeneous coupling, using NaOH	2041	[12]
Remazol Black 5	Chitosan/amino resin and chitosan bearing both amine and quaternary ammonium chloride moieties	625–932	[18]
Remazol Brilliant Orange 3R	GLA-crosslinked quaternary chitosan, heterogeneous coupling,	1060	[23]
Remazol Black 5	Acid-treated biomass of brown seaweed Laminaria sp.	102	[17]

Note: The maximum monolayer adsorption capacity (Q_m) is obtained from Langmuir isotherm equation.

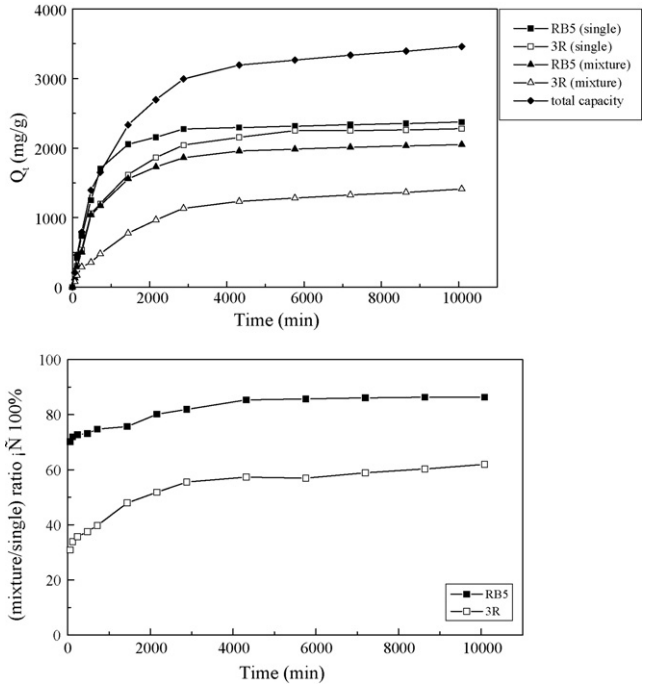

Fig. 7. (a) Absorption kinetics of the single and the mixture of RB5 and 3R on the ECH–RB5–NaOH microparticles (diameter: 149–250 μm) in 4.0 mM initial concentration of each dye at pH 3.0 and 30 °C. (b) The ratio of the adsorption capacity between the mixture solution and the single dye solution.

3.5. Regeneration

Fig. 8 shows the adsorption capacity of the RB5 dye on the ECH–RB5–NaOH microparticles in adsorption, desorption, and adsorption steps. The adsorption condition was at 4.0 mg/mL initial dye concentration, pH 3.0, and 30 °C. The desorption condition was at pH 10.0 of NaOH. The first adsorption step for 60 h reached the value of 2343 mg/g for the adsorption of the RB5 dye. The desorption step for 135 h was shown to have removed about 78.2% of the dye. This may be attributed to the fact that in the basic solution, the positively charged amino groups were deprotonated, and the electrostatic interaction between chitosan and dye molecules became much weaker [12]. At the same time, the adsorption of RB5 dye on the microparticles may be due to the dual nature of the process, physisorption and chemisorption, resulting in incomplete desorption (9,12). The second adsorption step for 135 h revealed to adsorb the dye again at about 74.4% of the first adsorption step. Therefore, the microparticles can be regenerated and reused for further dye adsorption.

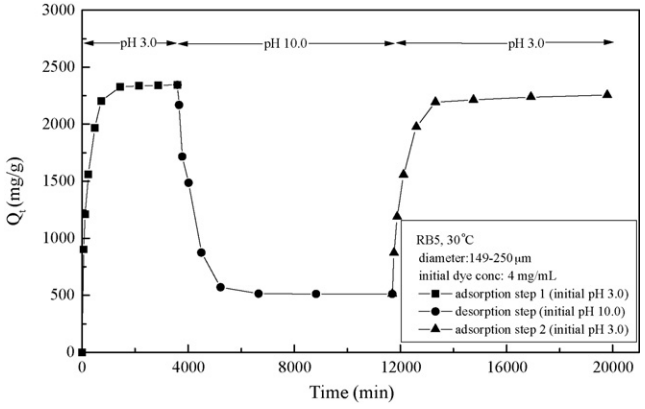

Fig. 8. Absorption and desorption of RB5 dye on the ECH–RB5–NaOH microparticles (diameter: 149–250 μm) at 4.0 mg/mL initial concentration of dyes and 30 °C with three steps: adsorption step 1 at pH 3.0, desorption step at pH 10.0 and adsorption step 2 at pH 3.0.

4. Conclusion

The templated crosslinked-chitosan microparticles prepared using the imprinting method with the RB5 dye as a template, ECH as a crosslinker and NaOH solution used for the microparticle formation showed the highest adsorption capacity for the RB5 dye compared with those using other methods with or without template, three crosslinkers, and two microparticle formations. The results showed that the adsorption of the RB5 dye on the microparticles was affected by the microparticle size, the initial dye concentration, the initial pH value, and the temperature. Both kinetics and thermodynamic parameters of the adsorption process were estimated. These data indicated an exothermic spontaneous adsorption process that kinetically followed the second-order adsorption process. Equilibrium experiments fitted well the Langmuir isotherm model and the maximum monolayer adsorption capacity for the RB5 dye was 2941 mg/g. In addition, the mean adsorption energy from the Dubinnin–Radushkevich isotherm revealed that the adsorption process might be due to the dual nature of the process, physisorption and chemisorption, and was predominant on the chemisorption process. The competition study showed that the adsorption of the RB5 dye on the microparticles in the mixture solution was much less affected by the existence of the 3R dye than the other way around. Furthermore, the templated microparticles could be regenerated through the desorption of the dye in pH 10.0 of NaOH solution and could be reused to adsorb the dye again.

Appendix A. Supplementary data

Supplementary data associated with this article can be found, in the online version, at doi:10.1016/j.jhazmat.2009.12.083.

References

[1] G. Crini, P.M. Badot, Application of chitosan, a natural aminopolysaccharide, for dye removal from aqueous solutions by adsorption processes using bath studies: a review of recent literature, Prog. Polym. Sci. 33 (2008) 399–447.
[2] I.T. Peternel, N. Koprivanac, A.M.L. Bozic, H.M. Kusic, Comparative study of UV/TiO_2, UV/ZnO and photo-Fenton processes for the organic reactive dye degradation in aqueous solution, J. Hazard. Mater. 148 (2007) 477–484.

[3] F.C. Wu, R.L. Tseng, R.S. Juang, Comparative adsorption of metal and dye on flake- and bead-types of chitosan prepared from fishery wastes, J. Hazard. Mater. B73 (2000) 63–75.
[4] F.C. Wu, R.L. Tseng, R.S. Juang, Enhanced abilities of highly swollen chitosan beads for color removal and tyrosinase immobilization, J. Hazard. Mater. B81 (2001) 167–177.
[5] S. Chatterjee, S. Chatterjee, S.B.P. Chatterjee, A.R. Das, A.K. Guha, Adsorption of a model anionic dye, ecosin Y, from aqueous solution by chitosan hydrobeads, J. Colloid Interface Sci. 288 (2005) 30–35.
[6] Z.G. Hu, J. Zhang, W.L. Chan, Y.S. Szeto, The sorption of acid dye onto chitosan nanoparticles, Polymers 47 (2006) 5838–5842.
[7] W.L. Du, Z.R. Xu, X.Y. Han, Y.L. Xu, Z.G. Miao, Preparation, characterization and adsorption properties of chitosan nanoparticles for eosin Y as a model anionic dye, J. Hazard. Mater. 153 (2008) 152–156.
[8] M.S. Chiou, H.Y. Li, Equilibrium and kinetic modeling of adsorption of reactive dye on crosslinked chitosan beads, J. Hazard. Mater. B93 (2002) 233–248.
[9] M.S. Chiou, H.Y. Li, Adsorption behavior of reactive dye in aqueous solution on chemical cross-linked chitosan beads, Chemosphere 50 (2003) 1095–1105.
[10] M.S. Chiou, P.Y. Ho, H.Y. Li, Adsorption of anionic dyes in acid solutions using chemically cross-linked chitosan beads, Dyes Pigments 60 (2004) 69–84.
[11] M.S. Chiou, G.S. Chuang, Competitive adsorption of dye metanil yellow and RB15 in acid solution on chemically cross-linked chitosan beads, Chemosphere 62 (2006) 731–740.
[12] A.H. Chen, S.M. Chen, Biosorption of azo dyes from aqueous solution by glutaraldehyde-crosslinked chitosans, J. Hazard. Mater. 172 (2009) 1111–1121.
[13] A.J. Varma, S.V. Deshpande, J.F. Kennedy, Metal complexation by chitosan and its derivatives; a review, Carbohydr. Polym. 55 (2004) 77–93.
[14] A.H. Chen, C.Y. Yang, C.Y. Chen, C.Y. Chen, C.W. Chen, The chemically crosslinked metal-complexed chitosans for comparative adsorptions of Cu(II), Zn(II), Ni(II) and Pb(II) ions in aqueous medium, J. Hazard. Mater 163 (2009) 1068–1075.
[15] R.M. Silverstein, F.X. Webster, D.J. Kiemle, Spectrometric Identification of Organic Compounds, 7th ed., John Wiley & Sons, New York, NY, USA, 2005, pp. 72–126.
[16] H. Yoshida, A. Okamoto, T. Kataoka, Adsorption of acid dye on crosslinked chitosan fibers: equilibria, Chem. Eng. J. 48 (1993) 2267–2272.
[17] K. Vijayaraghavan, Y.S. Yun, Biosorption of C.I. Reactive Black 5 from aqueous solution using acid-treated biomass of brown seaweed Laminaria sp., Dyes Pigments 76 (2008) 726–732.
[18] K.Z. Elwakeel, Removal of Reactive Black 5 from aqueous solutions using magnetic chitosan resins, J. Hazard. Mater. 163 (2009) 382–392.
[19] J. Tellinghuisen, Van't Hoff analysis of K^0 (T): how good or bad? Biophys. Chem. 120 (2006) 114–120.
[20] I. Langumuir, The adsorption of gases on plane surfaces of glass, mica and platinum, J. Am. Chem. Soc. 40 (1918) 1361–1403.
[21] H.M.F. Freundlich, Over the adsorption in solution, Z. Phys. Chem. A57 (1906) 358–471.
[22] S.P. Ramnani, S. Sabharwal, Adsorption behavior of Cr(VI) onto radiation crosslinked chitosan and its possible application for the treatment of wastewater containing Cr(VI), React. Funct. Polym. 66 (2006) 902–909.
[23] S. Rosa, M.C.M. Laranjeira, H.G. Riela, V.T. Favere, Cross-linked quaternary chitosan as an adsorbent for the removal of the reactive dye from aqueous solutions, J. Hazard. Mater. 155 (2008) 253–260.